Application of Explicit Finite-Difference Schemes in Two-Dimensional Modeling of Flows in Deformable Channels

Anatoly Krutov[1], Bakhadir Mirzaev[2], Dilshod Bazarov[2], Oybek Vokhidov[2]*, Abror Gadaev[3], Vladimir Kochetkov[4], Ikboloy Salimbaeva[2]

[1]State Oceanographic Institute, Moscow, Russia
[2]Tashkent Institute of Irrigation and Agricultural Mechanization Engineers, National Research University, Tashkent, Uzbekistan
[3]Samarkand State Architecture and Construction University named after Mirzo Ulugbek, Samarkand, Uzbekistan
[4]Research Institute of Power Engineering (RIPE "RusHydro"), Moscow, Russia
*Corresponding Author Email: o.voxidov@tiiame.uz

Abstract
Predicting the morphological evolution of river channels composed of easily erodible, fine-grained sediments is a recurring engineering problem, since many irrigation systems draw water through channels that are themselves prone to erosion and siltation. This paper presents a two-dimensional numerical model for simulating the morphological behavior of a river channel with a deformable bed. Sediment transport is described by a system of two-dimensional partial differential equations for the water–sediment mixture, expressing mass and momentum conservation in the form of the Saint-Venant equations, coupled with an explicit, grid-based scheme for bed and bank deformation that uses a minimal number of empirical coefficients. The model was tested against two independent sets of flume experiments - slope-leveling experiments at the Central Research Institute of Transport Construction (CRITC), and channel-quarry backfilling experiments at the State Hydrological Institute (SHI) - and its predictions were compared with the experimental data and with an independent numerical solution from the Research Institute of Power Engineering (RIPE). The proposed model reproduced the measured bed profiles with an accuracy comparable to, and in one case better than, the RIPE solution, with standard deviations from experimental data of 0.0019–0.0061 m across the tested time steps. The results demonstrate the significant contribution of bedload transport and the importance of interactions among water flow, sediment transport, and channel banks, while also indicating that, as with other models relying on empirical coefficients, further verification against field data is required.

Keywords: river channel morphology, Saint-Venant equations, numerical modeling, explicit finite-difference scheme, sediment transport, deformable channels

Introduction

The interaction between water flow and the underlying erodible surface plays a central role in numerous engineering problems, since it governs channel deformation, sediment transport, and deposition. Numerical modeling is one of the principal tools for addressing these problems, but modeling the interaction between water flow and the particles that compose a channel bed remains challenging because the relevant processes span a wide range of spatial and temporal scales. Bridging these scales within a single, computationally tractable model requires modeling methods that are simultaneously physically sound and efficient enough for routine engineering application. Studying these interactions deepens the understanding of flow–sediment–bank interactions and helps identify ways to optimize numerical methods for practical geotechnical and hydraulic engineering applications.

Numerical modeling of the hydrodynamic characteristics of flows in riverbeds and channels, whose principal methodological foundations were developed during the twentieth century, remains a widely used tool today. Continued refinement of these methods and expansion of their range of application (Belikov and Aleksyuk, 2020; Belikov, Borisova and Gladkov, 2010; Belikov, Zaytsev and Militeev, 2001; Gladkov, 1996; Krutov, 2019; Krutov, 1997; Lyakhter and Militeev, 1981; Militeev and Solovjov, 2017; Militeev and Solovyov, 2018a; Militeev and Solovyov, 2018b; Militeev and Krutov, 1980; Potapov, 2014; Andualem et al., 2023; Cundall and Strack, 1979; Hu et al., 2019; Kawaguchi, Tanaka and Tsuji, 1998) confirms that such methods are still far from a settled, final form: on the one hand they must yield numerical values of the sought quantities with the required accuracy, and on the other hand they must satisfy practical requirements of cost-effectiveness and computational efficiency. Nevertheless, as shown by more recent coupled particle–fluid approaches (Chen, Fraga and Liu, n.d.; Chou, Gu and Shao, 2015; Chou and Shao, 2016; Lu et al., 2023; Xu, Wang and Abegaz, 2025; Plenker and Grabe, 2016; Tao et al., 2021; Yazdanfar et al., 2021), there is a clear tendency to combine, within a single model, capabilities at different levels of detail—from the microlevel, where the characteristics of the interaction between particles carried by the flow are used to assess their impact on turbulent-flow characteristics, to the macrolevel, where flow parameters required for engineering calculations are obtained, including through the use of artificial intelligence (Tao et al., 2021). It should be noted that

models of this kind typically require specialized computing hardware or supercomputers for their implementation. At the same time, the development of numerical models that provide an adequate representation of processes occurring under real conditions, within a foreseeable computation time, using a minimum number of empirical coefficients, and on standard computers, continues (Belikov and Aleksyuk, 2020; Belikov, Zaytsev and Militeev, 2001; Krutov, 2019; Militeev and Solovjov, 2017; Militeev and Solovyov, 2018a).
The present study addresses this latter need. Its objective is to develop and test a two-dimensional numerical model, based on an explicit finite-difference scheme, that reproduces the morphological evolution of channels composed of easily erodible, fine-grained sediments with a minimum number of empirical constants, and to evaluate the model against independent flume experiments and an independently developed numerical solution.

Materials and Methods

Governing equations

Studies by Belikov and Aleksyuk (2020), Gladkov (1996) and Krutov (2019) have shown that, owing to the diversity and multifaceted nature of the factors influencing changes in the state of a water body, together with the requirement of adequately reflecting the processes involved, the task of assessing possible changes in riverbed morphology can only be solved by explicitly accounting for the hydrodynamic characteristics that govern these processes.
In addition to information on the hydraulic parameters of the flow, solving engineering problems related to sedimentation and erosion processes requires consideration of several further factors, including the concentration of suspended particles in the flow, their hydraulic size, and the lithology of the channel bed. Intensive economic use of water resources, combined with increasing volumes of water withdrawal, creates several challenges whose proper resolution determines not only the operational efficiency of hydraulic facilities but also their environmental safety. The most important of these are: water flow velocity fields; the content of suspended particles in the flow; and deformations of the flow bed.
For numerical calculations of flows with a deformable bottom, the system of two-dimensional Saint-Venant partial differential equations is proposed as the governing mathematical model, following the formulation described in detail by Krutov (1997) (Eqs. 1–3):

$$\frac{\partial h}{\partial t}+\frac{\partial (hu)}{\partial x}+\frac{\partial (hv)}{\partial y}=0 \tag{1}$$

$$\frac{\partial (hu)}{\partial t}+\frac{\partial}{\partial x}(hu2+gh^2/2)+\frac{\partial (huv)}{\partial y}=gh(S_{0x}-S_{fx}) \tag{2}$$

$$\frac{\partial (hv)}{\partial t}+\frac{\partial (huv)}{\partial x}+\frac{\partial}{\partial y}(hv2+gh^2/2)=gh\left(S_{0y}-S_{fy}\right) \tag{3}$$

where h is the water depth, u and v are the depth-averaged velocity components, Z_D is the channel bottom elevation, and g is the acceleration due to gravity. The friction stress vector at the bottom is collinear with the water-flow velocity vector, directed in the opposite direction, and determined by Darcy's formula (Eq. 4), in which the Darcy-Weisbach coefficient of hydraulic friction is determined by the Manning empirical formula (Eq. 5), where n is the dimensional roughness coefficient.

$$\tau_D=\frac{\rho\lambda}{8}|V|V \tag{4}$$

$$\lambda=\frac{2gn^2}{H^{\frac{1}{3}}} \tag{5}$$

As noted by Belikov and Aleksyuk (2020), Belikov, Zaytsev and Militeev (2001), Gladkov (1996) and Militeev and Solovyov (2018b), when calculating planned deformations it is necessary to consider the probability of bank soil erosion, including concentrated erosion, especially where the channel is composed of easily erodible soils. In such cases, the calculation separately determines the deformation of the bottom surface associated with the difference between the actual sediment content of the water flow and the transport capacity of the flow, together with the influence of sediment formed by bank and slope deformation. Calculation of the hydrodynamic model parameters by the explicit method proceeds stepwise:

1. Determining the maximum possible simulation time step that maintains calculation stability.
2. Calculating, in each computational cell, changes in the initial field variables (flow depth, velocity, and turbidity) at each time step, taking into account the inflow and outflow of water, the water mass balance, and compliance with the physical laws described by the system of equations (1–3).
3. Adjusting the bottom level of the calculation cell to account for changes in turbidity due to the influx and outflow of sediment, bottom erosion and sediment deposition, and slope creep.
4. When slopes slide, adjust the bottom level of the cells adjacent to the calculated one.
5. Updating the field variables accordingly.
6. Repeat the cycle from step 1 until the simulation time limit is reached.

The change in the bottom level in the calculation cell is (Eq. 6):

$$\frac{\Delta z_{d,x,y}}{\Delta t}=\frac{M_{fact}-M_{max}-M_{land}}{\rho_s\, d_x d_y\,(1-P)} \tag{6}$$

where M_{fact} is the mass of the actual sediment content in the water flow; M_{max} is the mass corresponding to the maximum transport capacity of the water flow; M_{land} is the mass of landslide material entering adjacent cells during slope deformation in the calculated cell; ρr is the bulk density of the soil; dx and dy are the linear dimensions of the cell; and P is the soil porosity coefficient. The mass of the actual sediment content in the calculation cell changes as sediment enters or leaves the cell with water exchanged with neighboring cells, and as material is added by slope sliding (Eq. 7):

$$\frac{\Delta M_{fact}}{\Delta t} = \sum_{i=1}^{4} S_i W_i + M_{trans} \tag{7}$$

where S_i and S_i are the sediment concentration and the volume of water supplied from the i-th neighboring cell during one calculation step, respectively, and M_{trans} is the portion of the soil mass converted into transported sediment by slope creep. The maximum mass of sediment that the water flow can transport in a calculation cell is (Eq. 8):

$$M_{max} = S_{max} * \rho_s * dx * dy * H \tag{8}$$

where S_{max} is the concentration corresponding to maximum saturation of the flow with sediment, dx and dy are the linear cell dimensions, and H is the water depth in the calculation cell. The Bagnold (1966) formula is used to calculate this saturation concentration (Eq. 9):

$$S_{max} = \alpha \frac{\rho_s}{(\rho_s - \rho_w)} \frac{\lambda V^2}{2gH} \left(\frac{0.13}{tg(\varphi) - I_{max,x,y}} + \frac{0.01V}{w} \right) \tag{9}$$

where α is the empirical coefficient of the intensity of sediment exchange between the bottom and the flow; ρ_s and ρв are the bulk densities of soil and water, respectively; λ is the coefficient of hydraulic friction, calculated using Manning's formula (Eq. 10); V is the velocity modulus (Eq. 11); tg(φ) is the tangent of the angle of internal friction of the soil; w is the average weighted hydraulic size of the soil; and $I_{max,x,y}$ is the maximum slope of the bottom of the calculation cell relative to its neighbors (Eq. 12).

$$\lambda = \frac{2gn^2}{H^{\frac{1}{3}}} \tag{10}$$

$$V = \sqrt{V_x^2 + V_y^2} \tag{11}$$

$$I_{max,x,y} = \max\left(I_{x-1,y}; I_{x+1,y}; I_{x,y-1}; I_{x,y+1}\right); \tag{12}$$

The slopes to the adjacent cells of the computational grid are determined by (Eq. 13), where Z_D denotes the cell bottom elevations:

$$I_{x\pm1,y} \left\{ \begin{array}{c} \frac{(Z_{d,x,y} - Z_{d,x\pm1,y})}{(d_x + d_{x\pm1})/2}, \ \text{at } Z_{d,x,y} > Z_{d,x\pm1,y} \\ \text{otherwise, not used (the bottom of the adjacent cell is higher)} \end{array} \right\} \tag{13a}$$

$$I_{x,y\pm1} \left\{ \begin{array}{c} \frac{(Z_{d,x,y} - Z_{d,x,y\pm1})}{(d_y + d_{y\pm1})/2}, \ \text{at } Z_{d,x,y} > Z_{d,x,y\pm1} \\ \text{otherwise, not used (the bottom of the adjacent cell is higher)} \end{array} \right\} \tag{13b}$$

A similar approach, using the bed slope within a computational cell rather than the overall channel bed slope, was proposed by Bailard and Inman (1981). The use of local slopes allows calculations to be performed for both flooded and coastal (partially dry) cells, thereby allowing the effects of rolling forces acting on particles located on submerged slopes to be taken into account.

When calculating landslide masses, the ultimate stable-slope hypothesis is used (Sokolovskiy, 1960). The calculation is performed in dry coastal cells having one or more (up to four) adjacent cells with a non-zero depth, using the principle of a horizontal bottom within each cell at the start and end of each calculation step. If the difference between the bottom elevation of the calculation cell and that of an adjacent wet cell exceeds the height of a stable slope, the soil pyramid on that side of the cell slides toward the adjacent cell. The excess of the bottom of the calculation cell over the bottom of each of its four adjacent cells is given by Eq. 14:

$$_{i=1}^{4}\Delta Z^*_{x,y,i} = Z_{d,x,y} - Z_{d,x\pm1,y\pm1} \tag{14}$$

If this excess is zero or negative, the creep on that side is not computed. If the slope height towards a given side exceeds the maximum height of a stable slope on that side, the slope slides down to the height of the stable slope, and the volume of soil subject to sliding is (Eq. 15):

$$W_i = d_x d_y (\Delta Z^*_{x,y,i} - H_{max,i}(1 - \frac{d_x}{3(d_x + d_{x+1})}) \tag{15}$$

where H_{max},i is the maximum height of a stable slope towards the i-th adjacent cell. The mass of the sliding pyramid on each adjacent side of the calculation cell is (Eq. 16):

$$M_{pyr,i} = \beta t \rho_s W_i \tag{16}$$

where β is an empirical coefficient, and t is the simulation time step. The maximum height of a stable slope is given by Eq. 17, where R_i is the distance between the centers of the calculated and the corresponding neighboring cell, and a is an auxiliary coefficient (Eq. 18) depending on the cohesion c, the volumetric weight γ, and the angle of internal friction φ of the water-saturated soil:

$$H_{max,i} = a\,\varepsilon_i + R_i\,tg(\varphi) \tag{17}$$

$$a = \frac{2\,c(1 + \sin(\varphi))}{\gamma\,(1 - \sin(\varphi))} \tag{18}$$

with the auxiliary terms ε_i (Eq. 19) and the relative coordinate of the center of the neighboring cell C_i (Eq. 20), where i is the serial number of the neighboring cell (from 1 to 4):

$$\varepsilon_i = \left(\frac{\pi}{2} - 1\right) \cdot e^{C_i}; \tag{19}$$

$$C_i = \frac{R_i}{a} \tag{20}$$

Because the scheme operates on the average weighted soil size, it is assumed that the fraction of sediment coarser than the average weighted size slides into neighboring cells, while the remainder stays in the cell as transported sediment. The mass of sediment sliding into adjacent cells is given by Eq. 21, and the mass of sediment in the calculation cell that is converted into transported sediment is given by Eq. 22, where $K_{coarse.sed.}$ is the proportion of the mass of coarse sediment depending on the granulometric composition:

$$M_{land,i} = K_{coarse.sed.} * M_{pyr,i} \tag{21}$$

$$M_{trans} = (1 - K_{coarse.sed.}) * \sum_{i=1}^{4} M_{pyr,i} \tag{22}$$

The corresponding change in the bottom level of the cells adjacent to the calculated one is given by Eq. 23:

$$\frac{\Delta z_{d,x\pm1,y}}{\Delta t} = \frac{M_{land,x\pm1,y}}{\rho_\pi d_{x\pm1} d_y (1-P)} \tag{23a}$$

$$\frac{\Delta z_{d,x,y\pm1}}{\Delta t} = \frac{M_{land,x,y\pm1}}{\rho_\pi d_x d_{y\pm1} (1-P)} \tag{23b}$$

Initial and boundary conditions

The initial conditions are the initial bottom surface $Z_D(x, y, 0)$ and the corresponding instantaneous fields of velocity $V(x, y, 0)$, depth $H(x, y, 0)$, and sediment concentration $S(x, y, 0)$. Boundary conditions at "solid" boundaries are no-flow conditions; at "fluid" boundaries, flow rates or water levels are typically specified; and at boundaries through which flow enters the computational domain, sediment concentration is specified. More complex boundary conditions are sometimes used, such as relations between flow rate and water level or "non-reflecting" boundary conditions.

Experimental data used for model testing

The proposed model was tested against the results of two independent sets of experimental studies: slope-leveling experiments conducted in the Hydraulics Laboratory of the Central Research Institute of Transport Construction (CRITC) (Belikov, Borisova and Gladkov, 2010), and channel-quarry backfilling experiments conducted at the State Hydrological Institute (SHI) (Gladkov, 1996).

The Central Research Institute of Transport Construction (CRITC) experiments were conducted in a flume with a variable slope and the following principal dimensions: length 18 m, width 2 m, and wall height 0.8 m. The longitudinal slope in the experiments was 0.0027. Water discharge was determined using a triangular weir located at the flume outlet. A sediment-collection pocket and a rocking shield for regulating the flume water level were installed at the end of the flume's working section. The erodible bed model was formed from sand with a grain-size distribution of $d_{av}{}^{g}$ = 0.24 mm and $K_{coarse.sed.}$= 0.366, as presented in Table 1.

Table 1. Fractional composition of sand in the model.

1–0.5 mm	0.5–0.25 mm	0.25–0.1 mm	<0.1 mm
0.2	31.9	67.7	0.2

Calculations were carried out using the software of Krutov, Kochetkov and Shkolnikov (2022) for the conditions reported by Belikov, Borisova and Gladkov (2010). The numerical model parameters α and β were selected during the calculation process on the basis of best agreement with the bed profile located 9.0 m from the start of the flume.

The State Hydrological Institute (SHI) experiments (Gladkov, 1996) on channel-quarry backfilling were carried out in a hydraulic flume 2.0 m wide and 50.0 m long with a sandy bottom. Sediment was supplied at the inlet boundary at a rate of 1.82 l/h ($S = 0.02$ kg/m³), with an average diameter of the supplied sediment of 0.32 mm and a flow rate of $Q = 40$ l/s. After a quasi-uniform regime was established, a channel quarry 0.7 m wide and 3.0 m long was excavated in the sandy bed; the quarry depth after excavation, before the start of the experiment, was approximately 14 cm below the average bed surface at its location.

For the quarry-backfilling simulations, a rectangular grid of 5,250 cells was constructed, similar to that used by the Research Institute of Power Engineering (RIPE). A roughness coefficient of 0.027 was adopted in the calculations, so that the steady-state water depths and velocities corresponded to the experimental data without the quarry present, namely an average depth of 8.8 cm and an average velocity of 22 cm/s. Calculations were then carried out with the quarry present; the best agreement with the experimental and Research Institute of Power Engineering (RIPE) results was obtained for $\alpha = 1.1$ and $\beta = 0.12$.

Results

For the Central Research Institute of Transport Construction (CRITC) slope-leveling experiments, the results of the proposed model were combined with the Central Research Institute of Transport Construction (CRITC) experimental data and the Research Institute of Power Engineering (RIPE) calculation results for the bed profile located 9.0 m from the start of the flume, at 1.5 and 5.5 hours after the start of the simulation (Figs. 1 and 2).

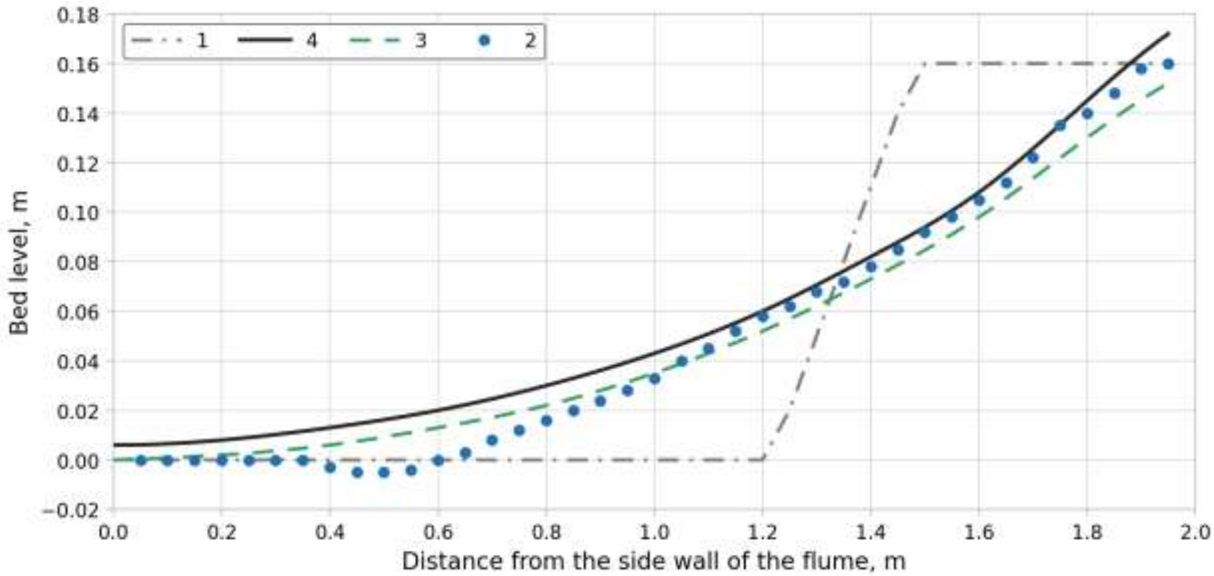

Fig. 1. Combined results of the CRITC experiment, the RIPE calculation, and the proposed model for a slope located 9.0 m from the start of the flume, at 1.5 hours from the start of the simulation. 1 – initial profile; 2 – CRITC experimental data; 3 – RIPE calculation; 4 – calculation using the proposed model.

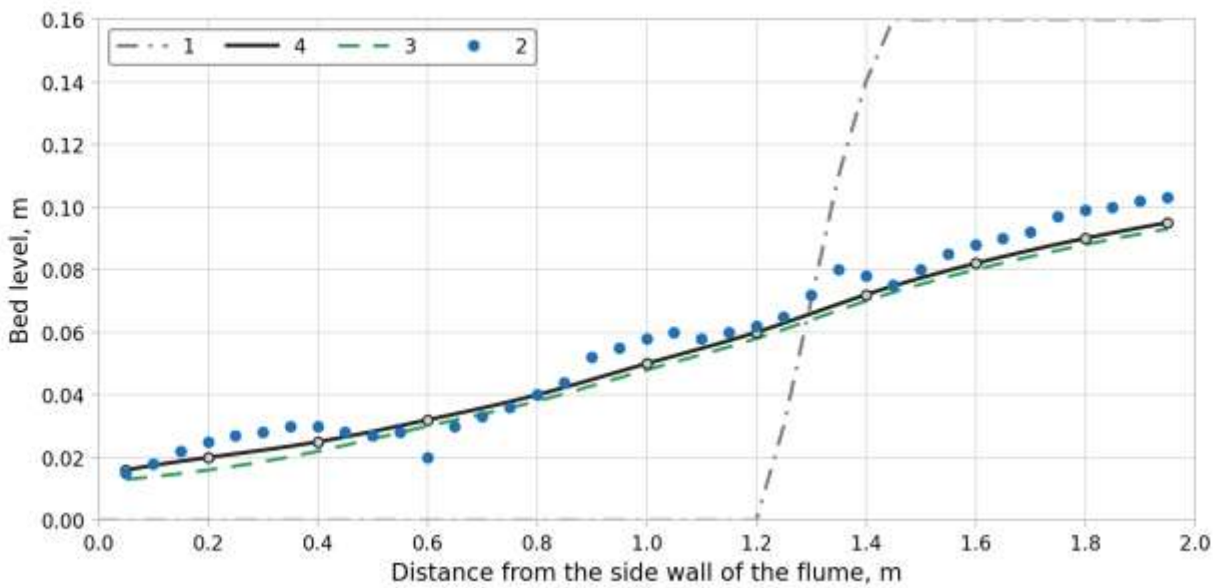

Fig. 2. Combined results of the CRITC experiment, the RIPE calculation, and the proposed model for a slope located 9.0 m from the start of the flume, at 5.5 hours from the start of the simulation. 1 – initial profile; 2 – CRITC experimental data; 3 – RIPE calculation; 4 – calculation using the proposed model.

The standard deviation of each modeling method from the experimental data, at 1.5 and 5.5 hours after the start of the experiment, is summarized in Table 2.

Table 2. Standard deviation of calculation results from experimental data (m).

Modeling method	**1.5 hours**	**5.5 hours**
RIPE calculation	0.0022	0.0026
Proposed model	0.0061	0.0019

For the SHI channel-quarry backfilling experiments, the comparison between the SHI experimental results, the RIPE calculation, and the proposed model at five successive times after the start of quarry development (21.2, 46.9, 73.8, 96.5, and 136.9 hours) is shown in Fig. 3.

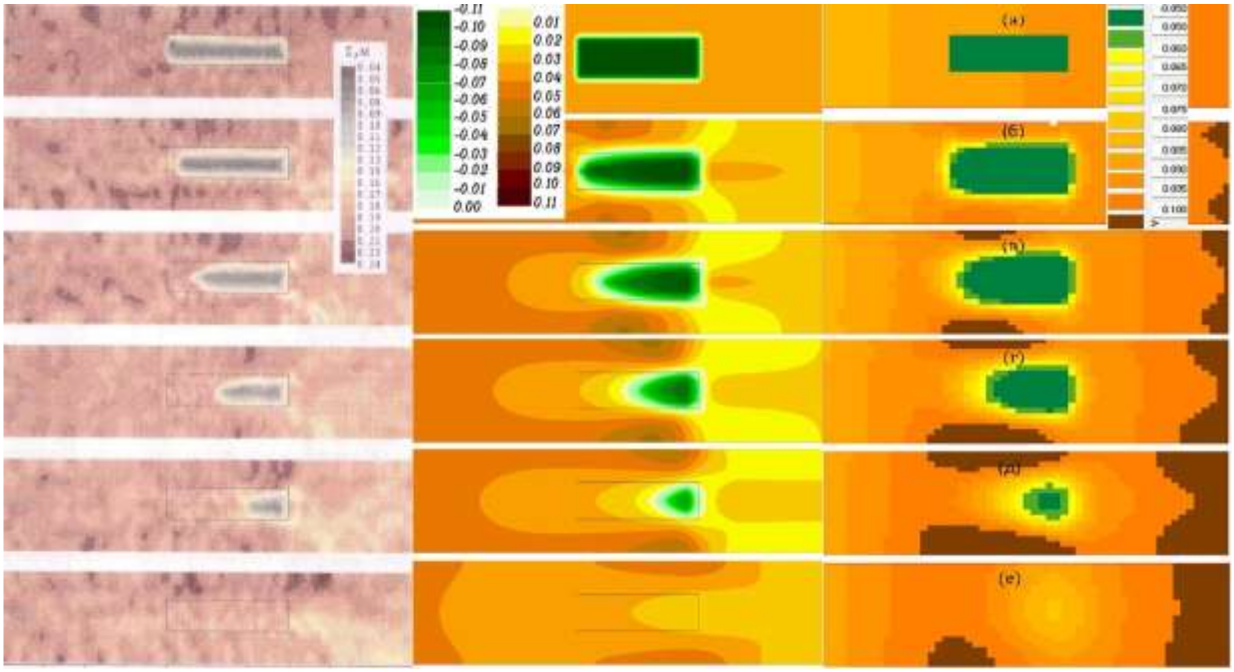

Fig. 3. Reformation of the bottom in the flume at the site of a single quarry during its filling: (a) bottom relief at the end of quarry development; (b–e) 21.2, 46.9, 73.8, 96.5, and 136.9 hours after quarry development, respectively. Left: SHI experimental results; center: RIPE calculation results; right: results of the calculation using the proposed model.

The calculation results using the proposed model showed almost complete qualitative and quantitative agreement with both the SHI experimental data and the independent RIPE calculation across the entire sequence of observation times (Fig. 3).

Discussion

The standard deviations obtained for the proposed model (0.0061 m at 1.5 hours and 0.0019 m at 5.5 hours; Table 2) are of the same order of magnitude as those obtained by the independently developed RIPE solution (0.0022 m and 0.0026 m, respectively), and are, in fact, smaller than the RIPE deviation at the later time step. Given that the proposed model uses an explicit, comparatively simple finite-difference scheme with a minimal number of empirical coefficients (α and β), while the RIPE solution represents an established, independently developed reference method, this level of agreement supports the suitability of the proposed model for practical engineering calculations of channel deformation in easily erodible, fine-grained sediments, without requiring specialized computing hardware.

The larger deviation of the proposed model at the earlier time step (1.5 hours; Table 2) relative to the later one (5.5 hours) suggests that the model requires a short initial adjustment period before its predictions stabilize relative to the observed bed evolution, consistent with the explicit scheme's stepwise adjustment of bed levels described above. This behavior should be taken into account when the model is applied to short-duration events, where the initial transient response may be relatively more important than in longer-duration simulations such as the quarry-backfilling case (up to 136.9 hours; Fig. 3), for which the agreement with both the SHI experimental data and the RIPE calculation remained close throughout the observation period.

These results are consistent with the general understanding, noted by Belikov and Aleksyuk (2020) and Belikov, Zaytsev and Militeev (2001), that bank and slope deformation in easily erodible channels must be treated as an integral part of the bed-deformation calculation rather than as a secondary correction; the explicit incorporation of the landslide and slope-creep terms (Eqs. 14–23) in the present model is consistent with this understanding and is reflected in the good agreement obtained for both the slope-leveling and quarry-backfilling test cases, which involve different balances between fluvial (flow-driven) and gravitational (slope-driven) sediment redistribution.

Compared with coupled particle-resolving approaches such as CFD-DEM (Chou, Gu and Shao, 2015; Chou and Shao, 2016; Lu et al., 2023; Xu, Wang and Abegaz, 2025), which explicitly resolve particle-scale interactions but require substantial computational resources, the present continuum-based, grid-averaged approach trades some physical resolution at the particle scale for the ability to run on standard computers within a foreseeable computation time - a property that is particularly relevant for routine engineering design, where many scenarios may need to be evaluated. The good agreement obtained here across two independent experimental datasets and an independent reference calculation indicates that this trade-off does not come at a substantial cost in predictive accuracy, at least for the sediment types and hydraulic conditions considered in these flume tests.

At the same time, the model relies on empirical coefficients (α, β, and the roughness coefficient n) that were calibrated against the same experimental datasets used for validation, which is a common limitation of models of this kind

(Belikov and Aleksyuk, 2020) and one that the model shares with the RIPE reference solution. The present tests were also conducted at flume scale, under controlled sediment supply and grain-size distributions; extrapolation to field-scale channels with heterogeneous, multi-fractional bed material and less-controlled boundary conditions has not been demonstrated here and would require independent verification against field data, as noted in the Conclusions below.

Conclusions

A numerical model is proposed for calculating the hydrodynamic characteristics of flows in channels composed of easily erodible soils. The model accounts for the non-uniformity and unsteadiness of the flow and uses a minimal number of empirical constants, making it suitable for describing processes of bed and bank deformation.

The proposed calculation method also allows the fractional composition of bottom sediments and transported sediments to be taken into account.

Comparison of the calculated results with experimental data from two independent flume studies, and with an independently developed reference solution, showed good qualitative and quantitative agreement, with standard deviations from experimental data in the range 0.0019–0.0061 m. However, like other models that rely on empirical constants, the proposed model requires careful verification using reliable field data before it can be applied with full confidence to field-scale channel morphodynamics.

Acknowledgement

The authors thank the Central Research Institute of Transport Construction (CRITC), the State Hydrological Institute (SHI), and the Research Institute of Power Engineering (RIPE) for the experimental and reference calculation data used to test the proposed model.

References

1. Andualem, T.G., Hewa, G.A., Myers, B.R., Peters, S. and Boland, J. (2023) Erosion and Sediment Transport Modeling: A Systematic Review. Land, 12, 1396.
2. Bagnold, R.A. (1966) An Approach to the Sediment Transport Problem from General Physics. US Geological Survey Professional Paper 422-I, Washington, D.C., 37 p.
3. Bailard, J.A. and Inman, D.L. (1981) An Energetic Bedload Model for a Plane Sloping Beach: Local Transport. Journal of Geophysical Research, 86, 2035-2043.
4. Belikov, V.V., Zaytsev, A.A. and Militeev, A.N. (2001) Numerical Modelling of Flow Kinematics in a Non-Erodible Channel Reach. Water Resources, 28, 701-710.
5. Belikov, V.V., Borisova, N.M. and Gladkov, G.L. (2010) Mathematical Model of Sediment Transport for Calculating the Siltation of Dredged Cuts and Channel Quarries. Journal of the University of Water Communications, 6, 105-113.
6. Belikov, V.V. and Aleksyuk, A.I. (2020) Shallow Water Models in River Hydrodynamics Problems. Russian Academy of Sciences, Moscow, 346 p.
7. Chen, B., Fraga, B. and Liu, Z. (n.d.) An Eulerian-Lagrangian Approach to Simulate Turbidity Currents. SSRN Electronic Journal.
8. Chou, Y.J., Gu, S.H. and Shao, Y.C. (2015) An Euler-Lagrange Model for Simulating Fine Particle Suspension in Liquid Flows. Journal of Computational Physics, 299, 955-973.
9. Chou, Y.J. and Shao, Y.C. (2016) Numerical Study of Particle-Induced Rayleigh-Taylor Instability: Effects of Particle Settling and Entrainment. Physics of Fluids, 28, 043302.
10. Cundall, P.A. and Strack, O.D.L. (1979) A Distinct Element Model for Granular Assemblies. Géotechnique, 29, 47-65.
11. Gladkov, G.L. (1996) Ensuring the Stability of Navigable River Channels During Dredging and the Development of Channel Quarries. Doctoral Dissertation, St. Petersburg State University of Water Communications, St. Petersburg.
12. Hu, D., Tang, W., Sun, L., Li, F., Ji, X. and Duan, Z. (2019) Numerical Simulation of Local Scour Around Two Pipelines in Tandem Using the CFD-DEM Method. Applied Ocean Research, 93, 101968.
13. Kawaguchi, T., Tanaka, T. and Tsuji, Y. (1998) Numerical Simulation of Two-Dimensional Fluidized Beds Using the Discrete Element Method (Comparison Between the Two- and Three-Dimensional Models). Powder Technology, 96, 129-138.
14. Krutov, A.N. and Militeev, A.N. (1980) A Numerical Method for Calculating Channel Deformations. Proceedings of the Symposium “Numerical Methods in Hydraulics,” Telavi.
15. Krutov, A.N. (1997) Development of the Theory and Methods for Predicting the Propagation of Pollutants in Surface Waters of Arid Zones. Doctoral Dissertation, State Oceanographic Institute, Moscow, 162 p.
16. Krutov, A.N. (2019) Results of Research on the Application of the Grid-Spectral Method for Predicting the Propagation of Pollutants in Reservoirs and Watercourses. State Oceanographic Institute, Moscow, Issue 218, 236-250.
17. Krutov, A.N. et al. (2021) Mathematical Modelling of Bottom Deformations in the Kinematic Wave Approximation. IOP Conference Series: Materials Science and Engineering, 1030, 012147.
18. Krutov, A.N., Kochetkov, V.V. and Shkolnikov, S.Y. (2022) Program for Calculating the Propagation of Long Waves

in Shallow Water Bodies of Arbitrary Configuration Considering Deformations of the Underlying Surface. Certificate of State Registration of Computer Programs No. 2022682252.
19. Krutov, A.N. (2023) Numerical Modelling of Long Waves in Wide Rectangular Channels in Lagrangian Coordinates. E3S Web of Conferences, 365, 03013.
20. Lu, Y., Liu, X., Sun, J., Xie, X., Li, D. and Guo, X. (2023) CFD-DEM Modeling of Turbidity Current Propagation in Channels with Two Different Topographic Configurations. Frontiers in Marine Science, 10, 1208739.
21. Lyakhter, V.M. and Militeev, A.N. (1981) Hydraulic Studies Using Numerical Methods. Water Resources, 1, 60-79.
22. Militeev, A.N. and Solovjov, V.A. (2017) Mathematical Modeling of River Channel Evolution in a Hydraulic System with Deformable Bottom. Journal of Applied Mechanics and Technical Physics, 58, 501-512.
23. Militeev, A.N. and Solovyov, V.A. (2018a) Numerical Simulation of Sediment Transport Processes Using the Divergent Form of the Saint-Venant Equations. Computational Continuum Mechanics, 11, 341-352.
24. Militeev, A.N. and Solovyov, V.A. (2018b) Methods for Calculating Channel Processes in Hydraulics Using Saint-Venant Equations. Proceedings of the Institute of Mechanics, Moscow State University, 24, 135-148.
25. Plenker, D. and Grabe, J. (2016) Simulation of Sand Particle Transport by Coupled CFD-DEM: First Investigations. Proceedings of the 8th International Conference on Scour and Erosion, Oxford, 12-15 September 2016, 109-118.
26. Potapov, I.I. (2014) Movement of Non-Cohesive Bedload Sediment. Computing Center of the Far Eastern Branch of the Russian Academy of Sciences, Khabarovsk, 58 p.
27. Sokolovskiy, V.V. (1960) Statics of Granular Media. 3rd Edition, Fizmatgiz, Moscow, 240 p.
28. Tao, H., Al-Khafaji, Z.S., Qi, C., Zounemat-Kermani, M., Kisi, O., Tiyasha, T. and Yaseen, Z.M. (2021) Artificial Intelligence Models for Suspended River Sediment Prediction: State-of-the-Art, Modeling Framework Appraisal, and Proposed Future Research Directions. Engineering Applications of Computational Fluid Mechanics, 15, 1585-1612.
29. Xu, J., Wang, F. and Abegaz, R. (2025) State of the Art of CFD-DEM Coupled Modeling and Its Application in Turbulent Flow-Induced Soil Erosion. Geosciences, 15, 21.
30. Yazdanfar, Z., Lester, D., Robert, D. and Setunge, S. (2021) A Novel CFD-DEM Upscaling Method for Prediction of Scour Under Live-Bed Conditions. Ocean Engineering, 220, 108442.